

independence of nuclear forces. These conclusions are summarized graphically in Fig. 3.

#### ACKNOWLEDGMENTS

The invaluable service of Professor D. J. Tendam and the cyclotron crew in maintaining the He<sup>3</sup> beam

during the course of these measurements is gratefully acknowledged. Discussions concerning various theoretical aspects of this work with Professor R. W. King have been of great value. B. T. Lucas is thanked for his aid in the reduction of data and servicing the experimental apparatus.

### Excited States in N<sup>14</sup> from the Elastic Scattering of Protons by C<sup>13</sup>†

E. KASHY,\* R. R. PERRY, R. L. STEELE,‡ AND J. R. RISSER

*Rice University, Houston, Texas*

(Received December 19, 1960)

Excited states in N<sup>14</sup> have been observed by measuring the differential elastic scattering cross section of C<sup>13</sup>(*p,p*)C<sup>13</sup> for proton energies from 2.6 to 5.0 Mev. Resonances were observed at proton energies of 2.743, 2.87, 3.105, 3.20, 3.78, 3.980, 4.04, and 4.14 Mev, corresponding to excited states in N<sup>14</sup> at 10.092, 10.21, 10.428, 10.52, 11.05, 11.240, 11.30, and 11.39 Mev, respectively. Single-level dispersion theory analysis indicates assignments  $J^\pi = 1^+(2^+)$ ,  $1^-$ ,  $2^+$ ,  $1^-$ ,  $1^+$ ,  $3^-$ ,  $2^-$ , and  $1^+$ , respectively, for these states. Analysis of previously published C<sup>13</sup>(*p,p*)C<sup>13</sup> data at lower energies confirms the assignments  $1^-$ ,  $0^+$ ,  $0^-$ ,  $3^-$ , and  $1^+$  for the states at 8.05, 8.61, 8.75, 8.90, and 8.98 Mev. A resonance at 4.265 Mev corresponding to the known narrow state at 11.504 Mev was not found in the elastic scattering data although it was found to be strong in C<sup>13</sup>(*p,p'*)C<sup>13\*</sup>.

THESE experiments were an extension of our experiments<sup>1</sup> with deuterons on C<sup>12</sup> involving a number of the same states in N<sup>14\*</sup>. The experimental techniques and method of analysis were essentially the same in the two experiments. States in N<sup>14\*</sup> at 11.05, 11.30, 11.39, and 11.504 Mev, which show clearly in C<sup>12</sup>(*d,d*)C<sup>12</sup>, C<sup>12</sup>(*d,p*<sub>0</sub>)C<sup>13</sup>, and/or C<sup>12</sup>(*d,p*<sub>1</sub>)C<sup>13\*</sup> at  $E_d = 0.92, 1.19, 1.31, \text{ and } 1.446$  Mev, have large proton partial widths to the ground and/or first excited state of C<sup>13</sup>. From the analysis of the deuteron data it was possible to make  $J^\pi$  assignments and estimate the proton partial widths. In addition, the results of the C<sup>12</sup>(*d,p*<sub>0</sub>)C<sup>13</sup> analysis imply the operation of selection rules other than those arising from the conservation of angular momentum and parity.<sup>2</sup> In view of the question of the validity of isotopic spin selection rules and the extensive interest<sup>3,4</sup> in the states of N<sup>14\*</sup>, it appeared important to check these results directly by elastic scattering of protons on C<sup>13</sup>. In taking the elastic scattering data, the range of energies was extended down to 2.6 Mev and up to 5.0 Mev. The states at

11.05, 11.30, and 11.39 Mev in N<sup>14\*</sup> produced resonances in C<sup>13</sup>(*p,p*)C<sup>13</sup> at  $E_p = 3.78, 4.04, \text{ and } 4.14$  Mev. Additional resonances at 2.743, 2.87, 3.105, 3.20, and 3.980 Mev corresponding to states in N<sup>14\*</sup> at 10.092, 10.21, 10.428, 10.52, and 11.240 Mev were observed in the elastic scattering data. A resonance due to the narrow 11.504-Mev state at  $E_p = 4.265$  Mev<sup>5</sup> was not observed in the elastic scattering data although it showed up strongly in C<sup>13</sup>(*p,p'*)C<sup>13\*</sup> ( $Q = -3.09$  Mev). Theoretical fits to the elastic scattering data were attempted, using dispersion theory in the single-level approximation. A preliminary report of this work has been given.<sup>6</sup>

Elastic scattering experiments with protons on C<sup>13</sup> in the range 0.4 to 1.6 Mev have been reported by Milne,<sup>7</sup> and in the range 1.6 to 3.3 Mev by Zipoy, Freier, and Famularo.<sup>8</sup> We have included in this paper a theoretical fit to the data of Milne, confirming his assignments. Extensive information on the states of N<sup>14\*</sup> has been accumulated through experiments on reactions.<sup>3</sup> Specific references will be given with the discussions of individual states where pertinent.

The ground state of C<sup>13</sup> has  $J^\pi = \frac{1}{2}^-$  and the character  $^2P_{\frac{1}{2}}$ . The elastic channel spin  $S$  can thus be 0 or 1 for protons on C<sup>13</sup>. As compared with C<sup>12</sup>(*d,d*)C<sup>12</sup> channel-spin-one scattering,<sup>1</sup> there is the added problem of the

† This work was supported in part by the U. S. Atomic Energy Commission.

\* Now at Department of Physics, Massachusetts Institute of Technology, Cambridge, Massachusetts.

‡ Now at Rocketdyne, Canoga Park, California.

<sup>1</sup> E. Kashy, R. R. Perry, and J. R. Risser, Phys. Rev. **117**, 1289 (1960).

<sup>2</sup> The  $p_0$  decay from the 11.05-, 11.30-, and 11.39-Mev states appears to be restricted to the channel-spin-zero mode.

<sup>3</sup> F. Aijzenberg-Selove and T. Lauritsen, Nuclear Phys. **11**, 1 (1959), and references in that paper.

<sup>4</sup> E. K. Warburton, H. J. Rose, and E. N. Hatch, Phys. Rev. **114**, 214 (1959), and references in that paper.

<sup>5</sup> The mass-equivalent energies given in reference 3 are used throughout.

<sup>6</sup> E. Kashy, R. R. Perry, and J. R. Risser, Bull. Am. Phys. Soc. **5**, 108 (1960).

<sup>7</sup> E. A. Milne, Phys. Rev. **93**, 762 (1954).

<sup>8</sup> D. Zipoy, G. Freier, and K. Famularo, Phys. Rev. **106**, 93 (1957).

channel-spin dependence of the scattering matrix. States with  $l_p = J \pm 1$ , i.e., states with  $J^\pi = 0^+, 1^-, 2^+, 3^-$ , etc., can be formed only from  $S=1$ . For all these states except  $0^+$  two  $l_p$  values are allowed, and transitions between the  $l_p$  values can occur in the scattering process. A  $0^-$  state can be formed only from  $S=0$  with  $l_p=0$ . The remaining states,  $1^+, 2^-, 3^+$ , etc., can be formed with only one value of  $l_p (=J)$  from both  $S=0$  and  $S=1$ .

At the lower end of the 2.6- to 5.0-Mev energy interval the elastic channel is the only particle channel open. A number of thresholds occur in the interval. The  $C^{13}(p,d)C^{12}$  threshold occurs at 2.93 Mev and the  $C^{13}(p,n)N^{13}$  threshold at 3.24 Mev in addition to the  $C^{13}(p,p')C^{13*}$  at 3.33 Mev. Below these thresholds the relative proton widths  $\Gamma_p/\Gamma$  are unity, effectively, since  $\Gamma_\gamma \ll \Gamma_p$ . Well above them, the  $\Gamma_p/\Gamma$  would be expected to be considerably less than one. The experimental results are consistent with this expectation. In the 4-Mev region, it would probably have been impossible from the elastic scattering data alone to have deduced the positions of the resonances and the  $J^\pi$  of the corresponding states. Above 4.3 Mev, although a number of states appear to be contributing to the cross section, no resonances are clearly enough indicated in the elastic scattering data to allow conclusions as to position or assignment.

#### EXPERIMENTAL PROCEDURE

The experiments were performed using the scattering chamber described previously.<sup>1</sup> The chamber was designed to use thin self-supporting foils<sup>9</sup> as targets. The protons were accelerated as atomic hydrogen ions in the Rice University 5.5-Mev Van de Graaff accelerator. The energy of the incident beam was determined using the  $90^\circ$  analyzing magnet which was calibrated in terms of a proton-moment magnetometer.

The chamber was fitted with two counters spaced at  $90^\circ$  in  $\phi$ , the angle about the chamber axis of rotation.<sup>1</sup> This in part explains the choice of angles in taking data. The elastic scattering data were taken at two sets of angles: (1) The backward counter was set at  $125.3^\circ$  c.m., the forward counter then being at  $38.3^\circ$  c.m.; (2) the forward counter was set at  $90.0^\circ$  c.m., the backward counter then being at  $165.5^\circ$  c.m. A single-channel pulse-height analyzer was used to take the data. The elastically scattered proton group was positioned in the wide channel of the single-channel analyzer with the aid of a 20-channel analyzer, which was kept connected in parallel with the single-channel analyzer. The position and width of the group as well as the magnitude of the background were monitored at each point with the 20-channel analyzer.

The principal difficulty lay in the subtraction of the  $C^{12}(p,p)C^{12}$  background in the elastic data. The elas-

tically scattered protons from the carbon isotopes were, of course, unresolvable. In addition to correction for the  $C^{12}$  content of the target, a correction had to be made for the buildup of a  $C^{12}$  deposit on the front face of the target by the proton beam. To establish a buildup correction, the first point of a run was repeated until  $N^{-1} < 0.005$ , where  $N$  was the total number of counts, and then taken again with equally large  $N$  at the end of the run. Total buildup for the run was calculated from the difference between these readings. The mass increment of  $C^{12}$  per point was then calculated on the assumption that the buildup took place at a uniform rate per point. Background subtractions proportional both to the  $C^{12}$  mass built up and to the  $C^{12}$  cross sections were then made.

For the purpose of  $C^{12}(p,p)C^{12}$  background subtraction, the  $C^{12}(p,p)C^{12}$  c.m. differential cross sections were calculated from the phase shifts<sup>10</sup> between 2.6 and 5.0 Mev at c.m. angles corresponding to the laboratory angles used in the elastic scattering experiments.<sup>11</sup> These in turn were converted to laboratory differential cross sections. Fortunately, these cross sections varied slowly with energy except in the immediate neighborhood of 4.8 Mev, where the resonant variation is so extreme that it was deemed impractical to make a background subtraction. In this region a gap was left in the plotted experimental data.

The experimental elastic scattering data were taken in essentially two parts. Thick targets enriched to 67%  $C^{13}$  were used first to establish the general level and gross structure of the cross section. Most of the experimental points outside the regions with narrow structure at 2.74, 2.86, and 3.98 Mev were obtained with these targets. A 180-microgram/cm<sup>2</sup> 67% target was used to obtain the data below 4.4 Mev in one series of runs, and another 416-microgram/cm<sup>2</sup> target of the same enrichment was used from 4.13 to 5.00 Mev in another series. The energy loss in the 180-microgram/cm<sup>2</sup> target varied from about 21 kev at 2.6 Mev to about 14 kev at 4.4 Mev; the energy loss in the 416-microgram/cm<sup>2</sup> target varied from about 34 kev at 4.1 Mev to 30 kev at 5.0 Mev. Since an absolute determination of the target thickness can not be made by weighing in the case of thin self-supporting foils,<sup>9</sup> the quoted target thicknesses were determined by counting scattered protons at energies and angles where both  $C^{12}$  and  $C^{13}$  elastic cross sections were known. For the 180-microgram/cm<sup>2</sup> target, counts were taken at 2.6 Mev over a range of forward angles, where the cross sections would be expected to be within a percent of the Rutherford cross sections. The target thickness was obtained from a fit to the angular distribution by taking the  $C^{13}$  cross sections equal to the Rutherford cross sections and

<sup>10</sup> C. W. Reich, G. C. Phillips, and J. L. Russell, Jr., Phys. Rev. **104**, 143 (1956).

<sup>11</sup> All calculations were carried out with phase shifts obtained from a large-scale graph in C. W. Reich's Ph.D. thesis, Rice Institute, 1956 (unpublished).

<sup>9</sup> E. Kashy, R. R. Perry, and J. R. Risser, Nuclear Instr. and Methods **4**, 167 (1959).

using  $C^{12}$  cross sections calculated from the phase shifts. The thickness of the 416-microgram/cm<sup>2</sup> target was determined by counting at 3.00 Mev and a laboratory angle of 165.0°, using a laboratory differential cross section of 73.6 mb/steradian for  $C^{12}$  obtained from the phase shifts and a laboratory cross section of 68.6 mb/steradian for  $C^{13}$  obtained from the reduced experimental data taken with the 180-microgram/cm<sup>2</sup> target. While the number of incident protons was known in terms of the integrated charge to the Faraday cup, and the solid angle subtended by the counter aperture at the beam spot position was known, all cross sections were actually determined in terms of a standard cross section by this procedure.

By the time the art of making very thin targets had been acquired, only material enriched to 37%  $C^{13}$  was available. A 23.0-microgram/cm<sup>2</sup> target of this material was used to take the elastic scattering data with the closely spaced experimental points in the regions of narrow structure at 2.74, 2.86, and 3.98 Mev. The proton energy loss in this target varied from 2.6 kev at 2.74 Mev to 2.0 kev at 3.98 Mev. The target thickness was determined by counting at 3.00 Mev and 165.0° laboratory angle, as described for the 416-microgram/cm<sup>2</sup> target.

It is difficult to assess the error in the differential cross sections. The error in calculating the  $C^{12}(p,p)C^{12}$  differential cross section from the phase shifts is estimated to be about 3%. The error in the experimental determination of target thickness and that due to the uncertainty in the  $C^{13}$  fractional content of the targets were probably also of this order. A reasonable estimate of the errors in the absolute elastic scattering cross sections appears to be  $\pm 10\%$ . Relative elastic scattering cross sections should in most cases be considerably more accurate. For example, since the  $C^{12}(p,p)C^{12}$  cross section varies slowly with energy except in the neighborhood of 4.8 Mev, the elastic scattering resonance

shapes should be quite accurately reproduced even though the absolute values of the cross-section differences are  $\pm 10\%$ .

Energies were obtained using the  $Li^7(p,n)Be^7$  threshold, the  $C^{13}(p,n)N^{13}$  threshold, the 4.265-Mev  $C^{13}(p,p')C^{13*}$  resonance, and the 4.808-Mev  $C^{12}(p,p)C^{12}$  resonance at 165° c.m. as calibration points of a scale proportional to  $f^2$ , where  $f$  was the frequency of the magnetometer proton-moment resonance. The uncertainty in the proton energy in our final data is estimated as  $\pm 5$  kev from 2.6 to 4.26 Mev and to increase to  $\pm 10$  kev at 5 Mev. The data points were plotted at the proton energy midway through the target. All the energies are laboratory-coordinate-system energies.

### ANALYSIS

Attempts to fit the elastic scattering data were made using dispersion theory in the single-level approximation. The method was essentially that described in reference 1 for the elastic scattering of deuterons from  $C^{12}$ . Equation (1) of that paper was the basis of the analysis. Using the notation of that paper,  $I=i=\frac{1}{2}$  so that  $S=1$  or 0. For  $S=0$ ,  $m_s=m_s'=0$ . There are thus three  $f_s^{m_s}$  to be evaluated since  $f_1^{+1}$  and  $f_1^{-1}$  are equal. In principle, Eq. (1) of reference 1 is inadequate for the more complicated problem of two values of the channel spin, since it contains no terms representing transitions between them. It was hoped, however, that the objective of obtaining  $J^\pi$  values could be accomplished without introducing these additional parameters. It chanced that a number of states that showed clearly in the elastic scattering data below 4 Mev belonged to the group  $0^+$ ,  $1^-$ ,  $2^+$ , etc., which could be formed only from  $S=1$ . Moreover, as a check on the analysis, we computed a fit to the data of Milne<sup>7</sup> in the 0.4- to 1.6-Mev region where only the elastic scattering channel is open. The results can be taken to indicate that the method is adequate.

We were unable to investigate completely the possibilities of the channel-spin dependence of the partial widths  $\Gamma_{lS}^{J^\pi}$ , which replace the  $\Gamma_l^{J^\pi}$  of the simpler problem. For the resonances at 3.78, 4.04, and 4.14 Mev, the  $\Gamma_{11}$  were taken equal to zero to be consistent with the  $C^{12}(d,p_0)C^{13}$  analysis.<sup>1</sup> Difficulties with the fits occurred in the 3-Mev region, where the assignments  $1^-$  and  $2^+$  restricted the channel spin to 1, and above 4.1 Mev. It therefore appears probable that the presence of unknown levels and low partial widths caused the difficulties rather than the shortcomings of the method of analysis.

The fits were obtained using an IBM 650 and later an IBM 704 computer. In the programs of Eq. (1) of reference 1, the terms independent of  $J$ , i.e., those containing  $\delta_{ll'}$  with phases involving  $\alpha_l$  and  $\phi_l$ , were independently summed, yielding the so-called "hard-sphere" part of the scattering amplitude. The "hard-sphere" phases  $\phi_l$  were not allowed to deviate greatly from the

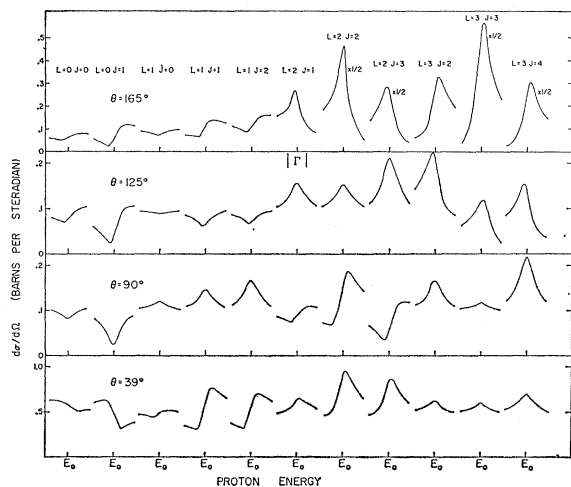


FIG. 1. Single-level curves for  $C^{13}(p,p)C^{13}$  calculated at 3.00 Mev with  $\phi_0 = -60^\circ$ ,  $\phi_1 = -15^\circ$ ,  $\phi_2 = -5^\circ$ ,  $\phi_l = 0$  for  $l > 2$ .

tabulated values of  $\tan^{-1}(F_l/G_l)$  on the assumption that anomalously large potential scattering would be expected to be  $J$  dependent and should be included by inserting resonant terms with large total widths. The values of  $\phi_l$  used in the fits to the elastic scattering data between 2.6 and 5.0 Mev were those given by the following expressions linear in  $E$ , the energy of the incident protons in Mev:

$$\begin{aligned}\phi_0 &= -17.64E - 10.0, \\ \phi_1 &= -5.88E + 9.3, \\ \phi_2 &= -0.555E - 2.05.\end{aligned}$$

In the fit to the Milne data:

$$\begin{aligned}\phi_0 &= -11E - 3, \\ \phi_1 &= -E.\end{aligned}$$

The first step in the analysis was to compute the line shape for each allowed combination of  $l$ ,  $J$ , and  $\pi$ . The results are shown in Fig. 1. The shapes were computed at 3.00 Mev with  $\phi_0 = -60^\circ$ ,  $\phi_1 = -15^\circ$ ,  $\phi_2 = -5^\circ$ , and  $\phi_l = 0$  for  $l > 2$ . Since space did not allow the display of the effect of varying the proportions of  $\Gamma_{l0}$  and  $\Gamma_{l1}$ , the  $\Gamma_{lS}/\Gamma$  were all taken equal to unity. For states that can be made with both channel spins and for pure elastic scattering, the extreme cross-section differences of Fig. 1 would be, for example, multiplied by  $\frac{3}{4}$  if  $\Gamma_{l1}/\Gamma$  were 1, and by  $\frac{1}{4}$  if  $\Gamma_{l0}/\Gamma$  were 1. We found it important to begin by computing single-level curves, since the line shapes sometimes allowed a decision to be made between  $J^\pi$  assignments and in many cases were a clue to the relative magnitudes of the partial widths associated with two possible  $l$  values.

## RESULTS

### 0.4- to 1.6-Mev Region

The results of the analysis of the Milne<sup>7</sup> data are shown in Fig. 2. The parameters used in the analysis are listed in Table I. The experimental points were taken from Figs. 3, 4, and 7 in Milne's paper. The  $J^\pi$  values confirm the assignments made by Milne, who reported a complete analysis only at the 0.55-Mev resonance. As a check on the method of analysis, the results are quite satisfactory since the computed cross

TABLE I. Parameters used in the analysis of the  $C^{13}(p,p)C^{13}$  data of Milne.<sup>a</sup>  $E_0^{J^\pi}$  and  $\Gamma$  in the table are on the laboratory energy scale.

$E(N^{14*})$ (Mev)	$E_0^{J^\pi}$ (Mev)	$J^\pi$	$\Gamma$ (kev)	$l$	$S$	$\Gamma_{lS}/\Gamma$
8.05	0.55	1 <sup>-</sup>	36	0	1	1.00
8.61	1.155	0 <sup>+</sup>	10	1	1	1.00
8.75	1.30	0 <sup>-</sup>	300	0	0	1.00
8.90	1.465	3 <sup>-</sup>	22	2	1	1.00
8.98	1.55	1 <sup>+</sup>	8	1	1	1.00

<sup>a</sup> See reference 7.

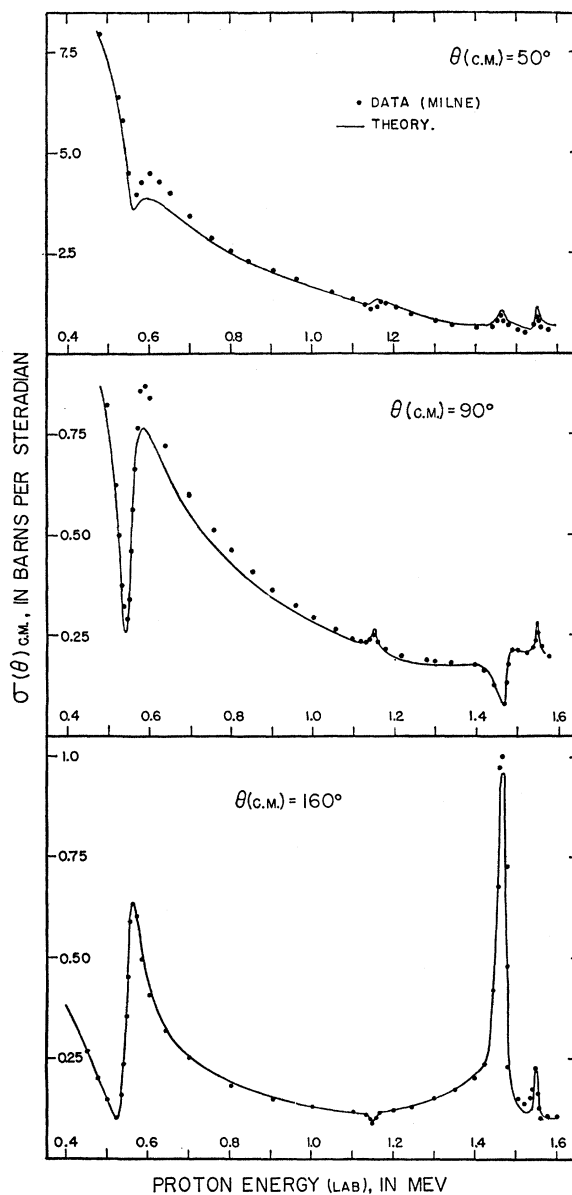


FIG. 2. Results of the analysis of the  $C^{13}(p,p)C^{13}$  data of Milne.<sup>7</sup> The experimental data were taken from Figs. 3, 4, and 7 of Milne's paper. The parameters used in the fit are listed in Table I.

sections are within the error range given by Milne:  $\pm 8\%$  for the forward to  $\pm 5\%$  for the backward angles.

### 2.6- to 5.0-Mev Region

The experimental differential elastic cross sections measured at c.m. angles  $39^\circ$ ,  $90^\circ$ ,  $125^\circ$ , and  $165^\circ$  from 2.6 to 5.0 Mev are shown in Fig. 3. The cross sections are in the center-of-mass system while the energies are laboratory bombarding energies midway through the target. The curves are fits obtained by the IBM 704 computer using Eq. (1) of reference 1 with the approximations discussed in the preceding section. The pa-

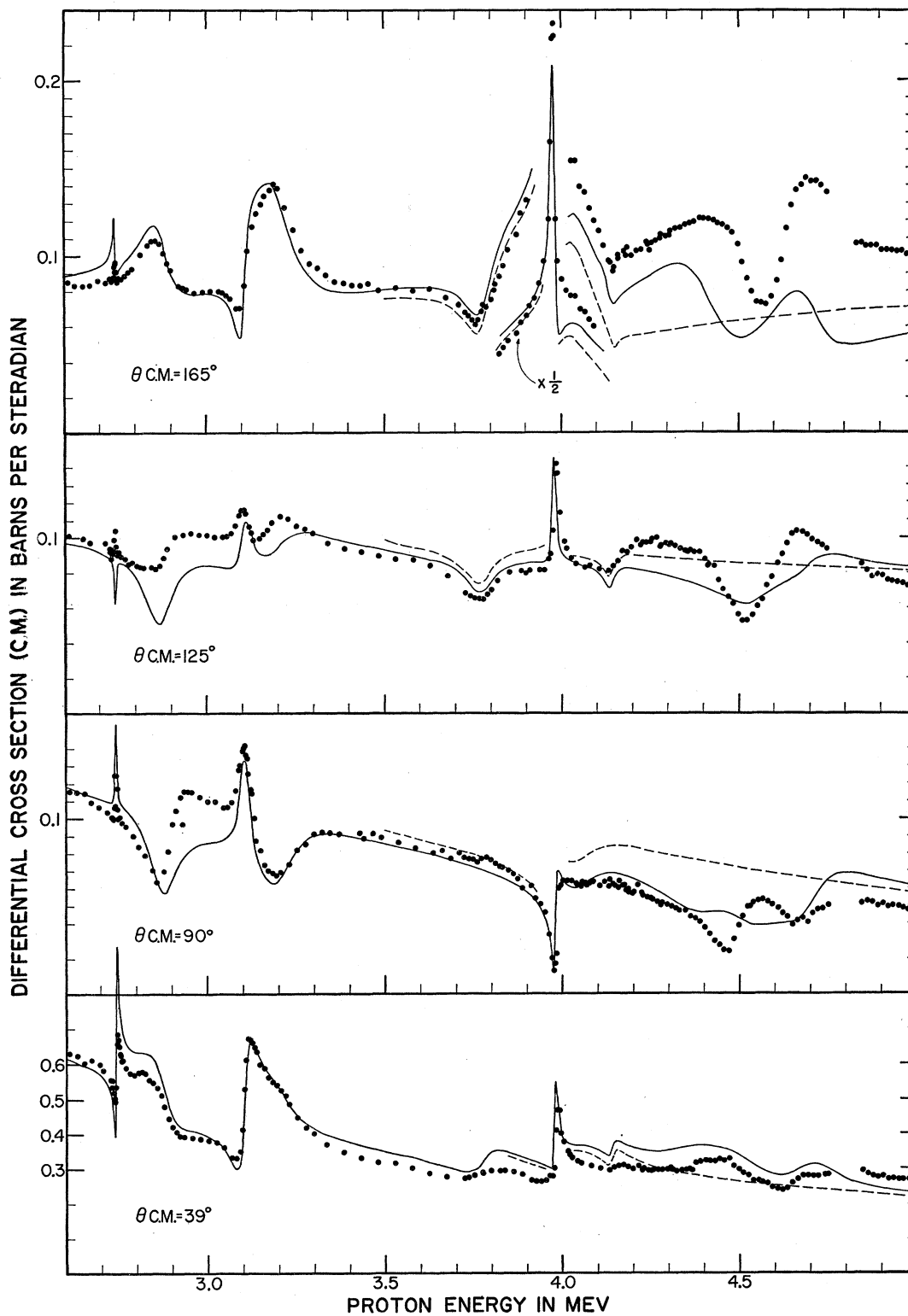


FIG. 3. The experimental  $C^{13}(p, p)C^{13}$  differential scattering cross sections at c.m. angles  $39^\circ$ ,  $90^\circ$ ,  $125^\circ$ , and  $165^\circ$  at laboratory bombarding energies from 2.6 to 5.0 Mev, together with single-level dispersion theory fits using the parameters of Table II and the values of  $\phi_l$  given in the text.

TABLE II. Parameters used in the fit to the C<sup>13</sup>(*p, p*)C<sup>13</sup> experimental differential elastic scattering cross sections from 2.6 to 5.0 Mev shown in Fig. 3.  $E_0^{J\pi}$  and  $\Gamma$  in the table are on the laboratory energy scale.

$E(N^{14*})$ (Mev)	$E_0^{J\pi}$ (Mev)	$J^\pi$	$\Gamma$ (kev)	$l$	$S$	$\Gamma_{lS}$
10.092	2.743	1 <sup>+</sup> (2 <sup>+</sup> )	5.5	1	0, 1	See discussion under Results
10.21	2.87	1 <sup>-</sup>	94	0, 2	1	$\Gamma_{01}=0.62\Gamma$ ; $\Gamma_{21}=0.38\Gamma$
10.428	3.105	2 <sup>+</sup>	38	1	1	$\Gamma_{11}=1.00\Gamma$ ; $\Gamma_{31}=0$
10.52	3.20	1 <sup>-</sup>	150	0, 2	1	$\Gamma_{01}=0.40\Gamma$ ; $\Gamma_{21}=0.60\Gamma$
11.05	3.78	1 <sup>+</sup>	100	1	0	$\Gamma_{10}=0.49\Gamma$ ; $\Gamma_{11}=0$
11.240	3.980	3 <sup>-</sup>	12	2	1	$\Gamma_{21}=0.86\Gamma$ ; $\Gamma_{41}=0$
11.30	4.04	2 <sup>-</sup>	196	2	0	$\Gamma_{20}=0.37\Gamma$ ; $\Gamma_{21}=0$
11.39	4.14	1 <sup>+</sup>	32	1	0	$\Gamma_{10}=0.27\Gamma$ ; $\Gamma_{11}=0$

Parameters of the resonances at 4.14 Mev and below as used in the fits of Fig. 3 are listed in Table II. Resonances were observed or must be postulated at 2.743, 2.87, 3.105, 3.20, 3.78, 3.980, 4.04, and 4.14 Mev. No satisfactory assignments could be made above 4.14 Mev, undoubtedly because of the density of states and the low proton elastic scattering partial widths. The assignments and widths will be discussed for the resonances individually in the paragraphs immediately following.

### 2.743-Mev Resonance

There is no doubt that the assignment must be  $J^\pi = 1^+$  or  $2^+$  as can be seen from the single-level shapes of Fig. 1. In the analysis of the assignment  $J^\pi = 1^+$  was used with  $\Gamma_{10} = \Gamma_{11} = \Gamma$ . If the experimental width and amplitude of the resonance are correctly given by Fig. 3, then the  $1^+$  assignment is correct, since  $\Gamma_{11}$  and  $\Gamma_{10}$  can be chosen for a quantitative fit with  $\Gamma_{11} + \Gamma_{10} = \Gamma$ , the proton channel being the only particle channel open. This is not true of the  $2^+$  assignment for which  $\Gamma_{10} = 0$  and  $\Gamma_{11} = \Gamma$ . However, the resonance must be investigated with extremely thin targets to rule out the  $2^+$  assignment. There is an additional difficulty of interference with background that is not quite reproduced in the fit. For example, the experimental points at  $125^\circ$  show a dispersion shape while the fit shows only a dip, a discrepancy that probably indicates the need of including in the analysis a broad state such as  $0^+$  made with the same  $l (= 1)$ .

### 2.87-, 3.105-, and 3.20-Mev Resonances

These three resonances interfere strongly. The assignments  $1^-$ ,  $2^+$ , and  $1^-$  are unambiguous. Since  $l = J$  is parity-forbidden at all three resonances, the states cannot be formed from the  $S = 0$  channel and the problem of the channel-spin dependence of the partial widths does not arise. However, all three states can be made with two  $l$  values, and a number of hours of computer time were devoted to fitting the data with the  $\Gamma_{lJ^\pi}$  taken in varying proportions. The parameters given in Table II for the fit of Fig. 3 were found superior to any other combination tried. The greatest discrepancy with the experimental data lies between

the 2.87- and 3.105-Mev resonances at about 3 Mev. No combination of parameters brought the calculated cross sections up nearer to the experimental at  $90^\circ$  and  $125^\circ$  just below 3 Mev without introducing peaks or dips at the resonances which were quite far outside experimental error. As mentioned in the discussion of the 2.743-Mev resonance, it is tempting to postulate a broad resonance due to a state of low  $J$ , such as a  $0^+$ , which could be seen only in its effect on the magnitude of the cross sections. No states with  $J = 0$  are listed in Table II although it seems reasonable to suppose that an interval two million volts wide would contain one or more. Some of the difficulty with the fit may arise from the use of a constant  $\Gamma$  for the 3.20-Mev resonance. The neutron threshold occurs 40 kev ( $\Gamma/4$ ) above the resonance energy, so that it might possibly improve the fit to use a smaller  $\Gamma$  below 3.24 Mev than is used above.

The  $2^+$  state at 10.428 Mev in N<sup>14\*</sup> corresponding to the 3.105-Mev resonance is undoubtedly the 10.43-Mev  $T = 1$  state corresponding to the capture resonance<sup>4,12</sup> in C<sup>13</sup>(*p, γ*)N<sup>14</sup> at this energy. According to Willard, Bair, Cohn, and Kington<sup>12</sup> the  $\gamma$ -ray data can only be explained with a  $2^+$  assignment if the state is formed with  $l = 3$ . In the elastic analysis a value of  $\Gamma_{31}$  larger than about  $0.05\Gamma$  results in a misfit at  $165^\circ$  which appears significant: Instead of a rounded top which characterizes the resonance in the experimental data in all runs, the fit exhibits a steep rise to a sharp break somewhat like the data at  $39^\circ$ . Perhaps a  $\Gamma_{31}/\Gamma$  approximately equal to 0.05 is sufficient to explain the C<sup>13</sup>(*p, γ*)N<sup>14</sup> cross section and angular distribution at this resonance. However, according to Warburton,<sup>13</sup> various relative values of  $\Gamma_{11}$  and  $\Gamma_{31}$  could account for the  $\gamma$ -ray data.

### 3.78-, 4.04-, and 4.14-Mev Resonances

These resonances correspond to the states at 11.05, 11.30, and 11.39 Mev in N<sup>14\*</sup> which are seen as resonances at  $E_a = 0.92, 1.19,$  and  $1.31$  Mev in C<sup>12</sup>(*d, d*)C<sup>12</sup> and C<sup>12</sup>(*d, p*)C<sup>13</sup>. There is no doubt that the fit to the C<sup>13</sup>(*p, p*)C<sup>13</sup> cross sections in Fig. 3 confirms the  $1^+$ ,  $2^-$ ,

<sup>12</sup> H. B. Willard, J. K. Bair, H. O. Cohn, and J. D. Kington, Phys. Rev. **105**, 202 (1957).

<sup>13</sup> E. K. Warburton, Phys. Rev. **113**, 595 (1959), p. 601.

and  $1^+$  assignment from the  $C^{12}(d,d)C^{12}$  analysis.<sup>1</sup> It would have been difficult or perhaps impossible to make the assignment from the elastic  $C^{13}(p,p)C^{13}$  data alone. The use of  $\Gamma_{11}=0$  in the fit of Fig. 3 likewise is confirmation of the conclusion from the  $C^{12}(d,p_0)C^{13}$  analysis that these states decay and therefore should be formed only by channel spin zero in the proton channel. In view of the shell model of the  $C^{13}$  ground state, channel-spin-zero states appear to be  $np$  triplet spin states. The conclusion that there are three such states close together is interesting. It would be interesting to determine the upper limits to the magnitudes of the  $\Gamma_{11}$  consistent with the elastic scattering data. The solid and dashed curves of Fig. 3 differ in the parameters of resonances included between 4.2 and 5 Mev. It is clear from comparison of the two curves that the fit over the 3.78-, 4.04-, and 4.14-Mev resonances is sensitive to the parameters of the resonances above 4.2 Mev, and that a quantitative fit over the whole energy interval is needed to determine the upper limits of the  $\Gamma_{11}$ . Nevertheless, because of the relative statistical weights  $(2S+1)$  of the two channel spins, magnitudes of the  $\Gamma_{11}$  approximately the same as those of the  $\Gamma_{10}$  are ruled out, as can be seen by comparison with the cross sections of Fig. 1.

### 3.980-Mev Resonance

The state with  $J^\pi=3^-$  corresponding to this narrow resonance can be formed only by channel spin 1. There can be no interference with the broad  $2^-$  state corresponding to the 4.04-Mev resonance if the latter can be formed only by channel spin zero. The experimental cross sections appear to be additive. The fact that this state does not show up as a resonance in  $C^{12}(d,p_0)C^{13}$  could possibly mean that  $T=1$ , but the argument is weak since the deuteron partial width would be expected to be small because of the barrier for a 1-Mev deuteron with  $l=3$ .

### 4.265-Mev Resonance

Attempts to detect a resonance in the elastic scattering cross section at this energy failed, although the resonance was found with a peak cross section of some 20 mb in the inelastic scattering reaction  $C^{13}(p,p')C^{13*}$  ( $Q=-3.09$  Mev).

### 4.2- to 5.0-Mev Region

The dashed curve of Fig. 3 represents a fit calculated on the assumption that there are no resonances above 4.14 Mev, and the solid curve on the assumption that there are three resonances at 4.40, 4.53, and 4.70 Mev, due, respectively, to states with  $J^\pi=1^-$  ( $\Gamma=240$  kev,  $\Gamma_{01}=0.2$ ,  $\Gamma_{21}=0.6$ ),  $J^\pi=0^-$  ( $\Gamma=160$  kev,  $\Gamma_{00}=0.64$ ), and  $J^\pi=1^-$  ( $\Gamma=160$  kev,  $\Gamma_{01}=0.20$ ,  $\Gamma_{21}=0.64$ ). The assignments are clearly wrong. The difficulty lies partly in the fact that the experimental evidence<sup>3</sup> on the number, positions, and widths of the resonances is somewhat conflicting and partly in the absence of quantitative estimates of reaction partial widths, which can only be obtained from fairly complete knowledge of the energy dependence of total reaction cross sections. Information on the detailed energy dependence of the  $C^{13}(p,n)N^{13}$  total cross section would be especially desirable.

### Reduced Widths

The reduced widths for proton emission of the states in Table II were calculated and all found to be of the order of a percent of the Wigner limit.

### ACKNOWLEDGMENTS

We wish to acknowledge the courtesy of the Shell Development Company for allowing us to use their IBM 650 computer and of The Texas Engineering Experiment Station Data Processing Center for the use of their IBM 704 computer.